

SPECTRAL ELEMENT METHODS ON HYBRID TRIANGULAR AND QUADRILATERAL MESHES

JINGLIANG LI, HEPING MA, LI-LIAN WANG, AND HUA WU

In memory of Professor Benyu Guo

Abstract. In this paper, we implement and analyse a spectral element method (SEM) on hybrid triangular and quadrilateral element meshes, where the elemental transformation between the triangular element and the reference element is based on the mapping in [17]. We introduce the notion of “quasi-interpolation” to glue the hybrid elements which can build in the singularity of the elemental mapping, and only affects one coefficient of the tensorial nodal basis expansion. Therefore, the hybrid method can be implemented as efficiently as the usual quadrilateral SEM. We also rigorously analyse the “quasi-interpolation” error and the convergence of the hybrid SEM, which show the spectral accuracy can be kept.

Key words. Triangle-rectangle mapping, spectral element method, polygon domain

1. Introduction

The spectral element method, which enjoys both high accuracy of the spectral method and geometric flexibility of the finite element method, has become a powerful tool, perhaps the method of choice, for challenging simulations with stringent accuracy and storage requirement (see, e.g., [19, 5, 13, 2]). The quadrilateral/hexahedral spectral element method (QSEM) has been studied and documented well in literature. We particularly highlight that Guo and Jia [12, 8] conducted a very delicate analysis of the quadrilateral SEM, where the error estimates were featured with the explicit dependence of the geometric parameters of the elements, and where the so-called “quasi-orthogonal projections” played an important part in the analysis. The results therein could provide deep insights into how the quality of the mesh affects the accuracy of spectral element approximations.

It is known that the triangular/tetrahedral spectral element method (TSEM) on unstructured meshes has more flexibility for complex computational domains and adaptivity techniques. Considerable efforts have been devoted to these approaches along the lines: (i) nodal TSEM based on high-order polynomial interpolation on special interpolation points [3, 11, 26]; (ii) modal TSEM based on the Koornwinder-Dubiner (KD) polynomials [14, 6, 13, 15, 21]; and (iii) approximation by non-polynomial functions [23, 16, 4]. It is noteworthy that due to lacking of tensorial structure, these approaches are much more complicated in implementation than QSEM.

One of the main purposes of this work is to further the study of Guo and Jia [7, 8] by considering the scenario when some of the quadrilateral elements deform into triangular elements. Indeed, using hybrid triangular and quadrilateral elements, one can handle more complex domains with more regular meshes, e.g., by tiling the triangular elements along the boundaries of complex obstacles. In practice, one also wishes the implementation of such a hybridisation can inherit the tensorial structure of the QSEM. It is noted that the constants in the error estimates depend on the

lower bound of $1/J$ (J is the Jacobian of the mapping from a quadrilateral element to the reference square, see [12, (2.9)]). Thus, the constants in the upper bounds become infinity when one of the interior angles is close to π , i.e., the quadrilateral element deforms into a triangular element. This brings about an interesting issue: How to effectively treat singular deformations in implementation without loss of accuracy and rigorously analyse the approach?

The tackle of the issue essentially relies on the triangle-rectangle transformation reported in [17]. The mapping pulls one side (at the middle point) of the triangle to two sides of the rectangle, and results in desirable distributions of the grids, compared with the Duffy mapping [6]. Samson et al [20] proposed a modal approach based on the inspection that the product of any continuous function and $1/J$ is integrable over the reference square, so the singularity of the elemental transformation can be perfectly removed. However, much care is needed for the implementation. Indeed, the nodal basis is more preferable in practice.

In this paper, we introduce the so-called “quasi-interpolation” to glue the neighbouring triangles and rectangles in C^0 -sense. Different from the usual tensorial interpolation, this interpolation builds in the “pole” condition of the singular transformation. This however only affects one interpolation coefficients which should be pre-determined by some other coefficients. Therefore, we can incorporate this “known” equation in the implementation leading to a minimal amendment of usual QSEM codes. It is noteworthy that this notion is different from the “quasi-orthogonal projection” [12], which was essentially intended to glue and analyse the modal approach for QSEM by separating interior, boundary and vertex modes. We also conduct error analysis of the “quasi-interpolation” and hybrid SEM, and derive the estimates following the spirit of Guo and Jia [12] in terms of showing the explicit dependence of some important parameters.

The rest of the paper is organised as follows. In Section 2, we start with the elemental transformations between quadrilaterals, and the triangle-rectangle mapping. More importantly, we study the situation when one quadrilateral element gradually deforms into a triangular element, and examine how the accuracy is deteriorated and conditioning of the system unpleasantly grows. In Section 3, we introduce the “quasi-interpolation” and derive its interpolation error estimate. In Section 4, we implement the hybrid SEM for elliptic and Stokes problems, conduct some related analysis, and provide various numerical results to show the accuracy.

2. Preliminaries

In this section, we first present the transformation \mathbf{F}_\square , which transforms the reference square to a convex quadrilateral. Then we test the changes in effect of applying the standard QSEM to elliptic problems when a convex quadrilateral deforms to a triangle gradually. At last, we present the limited transformation \mathbf{F}_\triangle , which transforms the reference square to a triangle, and find out what makes the standard QSEM out of operation when handling the triangular element.

2.1. Elemental transformation between quadrilaterals. Let (ξ, η) be the coordinate system related to the reference square $\square := \Lambda_\xi \times \Lambda_\eta = (-1, 1)^2 = \Lambda^2$. Denote by Q a generic convex quadrilateral with vertices $\{Q_j : (x_j, y_j)\}_{j=1}^4$ in (x, y) -coordinates. For clarity of presentation, we use boldface letters to denote vectors or vector-valued functions throughout this paper, e.g.,

$$(1) \quad \mathbf{x} = (x, y), \quad \mathbf{x}_j = (x_j, y_j), \quad \mathbf{a}_j = (a_j, b_j), \quad 1 \leq j \leq 4.$$

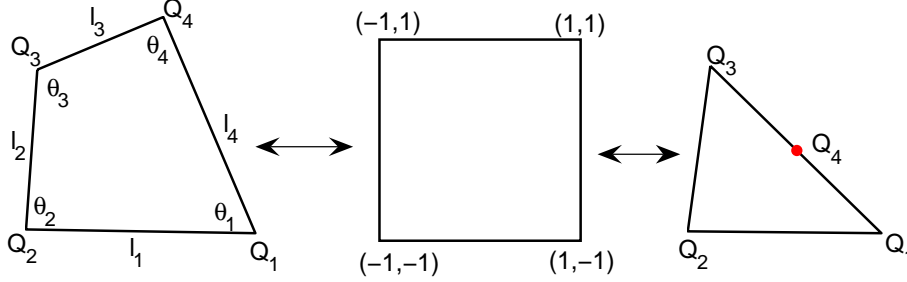


FIGURE 1. Left pair: elemental transformation between Q and \square .
Right pair: elemental transformation between \triangle and \square .

Recall the bilinear transformation $\mathbf{F}_{\square} : \square \rightarrow Q$ given by

$$(2) \quad \mathbf{x} = \mathbf{x}(\xi, \eta) = \mathbf{F}_{\square}(\xi, \eta) := \sum_{j=1}^4 \mathbf{x}_j \sigma_j(\xi, \eta) = \mathbf{a}_1 + \mathbf{a}_2 \xi + \mathbf{a}_3 \eta + \mathbf{a}_4 \xi \eta,$$

for all $(\xi, \eta) \in \bar{\square}$, where

$$(3) \quad \begin{aligned} \sigma_1 &= \frac{1}{4}(1 + \xi)(1 - \eta), & \sigma_2 &= \frac{1}{4}(1 - \xi)(1 - \eta), \\ \sigma_3 &= \frac{1}{4}(1 - \xi)(1 + \eta), & \sigma_4 &= \frac{1}{4}(1 + \xi)(1 + \eta), \end{aligned}$$

and

$$(4) \quad \begin{aligned} \mathbf{a}_1 &= (\mathbf{x}_1 + \mathbf{x}_2 + \mathbf{x}_3 + \mathbf{x}_4)/4, & \mathbf{a}_2 &= (\mathbf{x}_1 - \mathbf{x}_2 - \mathbf{x}_3 + \mathbf{x}_4)/4, \\ \mathbf{a}_3 &= (-\mathbf{x}_1 - \mathbf{x}_2 + \mathbf{x}_3 + \mathbf{x}_4)/4, & \mathbf{a}_4 &= (-\mathbf{x}_1 + \mathbf{x}_2 - \mathbf{x}_3 + \mathbf{x}_4)/4. \end{aligned}$$

The correspondence between the vertices of Q and \square is illustrated in FIG. 1 (e.g., $Q_1 \leftrightarrow (1, -1)$). Note that if Q is a rectangle, then $\mathbf{a}_4 = 0$ and \mathbf{F}_{\square} simplifies to the linear transformation:

$$(5) \quad \mathbf{x} = \mathbf{x}(\xi, \eta) = \mathbf{a}_1 + \mathbf{a}_2 \xi + \mathbf{a}_3 \eta.$$

The Jacobian matrix of the transformation and its inverse are

$$(6) \quad \mathbb{J}_{\square} = \begin{bmatrix} \partial_{\xi} \mathbf{x} \\ \partial_{\eta} \mathbf{x} \end{bmatrix} = \begin{bmatrix} \mathbf{a}_2 + \mathbf{a}_4 \eta \\ \mathbf{a}_3 + \mathbf{a}_4 \xi \end{bmatrix}, \quad \mathbb{J}_{\square}^{-1} = \frac{1}{J_{\square}} \begin{bmatrix} b_3 + b_4 \xi & -(b_2 + b_4 \eta) \\ -(a_3 + a_4 \xi) & a_2 + a_4 \eta \end{bmatrix},$$

where $J_{\square} = \det(\mathbb{J}_{\square})$ is the Jacobian determinant. Note that J_{\square} is a linear function in ξ, η , and it attains its extremum at four vertices of \square (see [25, 7]):

$$(7) \quad \begin{aligned} J_{\square}^{\min} &:= \min_{(\xi, \eta) \in \bar{\square}} J_{\square}(\xi, \eta) = \min \{J_{\square}(-1, -1), J_{\square}(1, -1), J_{\square}(-1, 1), J_{\square}(1, 1)\}, \\ J_{\square}^{\max} &:= \max_{(\xi, \eta) \in \bar{\square}} J_{\square}(\xi, \eta) = \max \{J_{\square}(-1, -1), J_{\square}(1, -1), J_{\square}(-1, 1), J_{\square}(1, 1)\}, \end{aligned}$$

where the values of J_{\square} at four vertices can be evaluated explicitly. In particular,

$$(8) \quad J_{\square}(1, 1) = \{(x_3 - x_4)y_1 + (x_1 - x_3)y_4 + (x_4 - x_1)y_3\}/4.$$

Moreover, we have (see [25]):

$$(9) \quad \begin{aligned} J_{\square}(1, -1) &= l_1 l_4 \sin \theta_1, & J_{\square}(-1, -1) &= l_1 l_2 \sin \theta_2, \\ J_{\square}(-1, 1) &= l_2 l_3 \sin \theta_3, & J_{\square}(1, 1) &= l_3 l_4 \sin \theta_4. \end{aligned}$$

Note that for a convex quadrilateral Q , we have $\theta_j \in (0, \pi)$ for $1 \leq j \leq 4$. Therefore, J_\square is positive and

$$(10) \quad 0 < J_\square^{\min} \leq J_\square(\xi, \eta) \leq J_\square^{\max}, \quad \forall (\xi, \eta) \in \bar{\square}.$$

Given any $u(x, y)$ on Q , we define the transformed counterpart on \square as $\tilde{u}(\xi, \eta) = (u \circ \mathbf{F}_\square)(\xi, \eta)$. Let $\nabla = (\partial_x, \partial_y)^t$ and $\tilde{\nabla} = (\partial_\xi, \partial_\eta)^t$ be the gradient operators. It is clear that we have

$$(11) \quad \tilde{\nabla} \tilde{u} = \mathbb{J}_\square \nabla u, \quad \nabla u = \mathbb{J}_\square^{-1} \tilde{\nabla} \tilde{u},$$

For notational convenience, we introduce the differential operators

$$(12) \quad \begin{aligned} \tilde{\nabla}_a &= -(a_3 + a_4)\partial_\xi + (a_2 + a_4)\partial_\eta, & \tilde{\nabla}_b &= (b_3 + b_4)\partial_\xi - (b_2 + b_4)\partial_\eta, \\ \tilde{\nabla}_* &= (1 - \xi)\partial_\xi - (1 - \eta)\partial_\eta. \end{aligned}$$

Thus, the gradient operator on Q can be rewritten as

$$(13) \quad \nabla u = \frac{1}{J_\square} (\tilde{\nabla}_b - b_4 \tilde{\nabla}_*, \tilde{\nabla}_a + a_4 \tilde{\nabla}_*)^t \tilde{u} := \hat{\nabla} \tilde{u}.$$

Accordingly, for any $u, v \in H^1(Q)$, we have

$$(14) \quad \begin{aligned} (\nabla u, \nabla v)_Q &= \iint_\square \hat{\nabla} \tilde{u} \cdot \hat{\nabla} \tilde{v} J_\square d\xi d\eta = \iint_\square J_\square^{-1} (\tilde{\nabla}_a \tilde{u} \tilde{\nabla}_a \tilde{v} + \tilde{\nabla}_b \tilde{u} \tilde{\nabla}_b \tilde{v}) d\xi d\eta \\ &\quad + \iint_\square J_\square^{-1} (a_4 \tilde{\nabla}_* \tilde{u} \tilde{\nabla}_a \tilde{v} + a_4 \tilde{\nabla}_* \tilde{v} \tilde{\nabla}_a \tilde{u} - b_4 \tilde{\nabla}_* \tilde{u} \tilde{\nabla}_b \tilde{v} - b_4 \tilde{\nabla}_* \tilde{v} \tilde{\nabla}_b \tilde{u}) d\xi d\eta \\ &\quad + \iint_\square J_\square^{-1} (a_4^2 + b_4^2) \tilde{\nabla}_* \tilde{u} \tilde{\nabla}_* \tilde{v} d\xi d\eta, \end{aligned}$$

and

$$(15) \quad (u, v)_Q = (\tilde{u}, J_\square \tilde{v})_\square = \iint_\square \tilde{u} \tilde{v} J_\square d\xi d\eta.$$

2.2. An illustration of singularity of a deformed quadrilateral element.

To motivate our algorithm development in next section, we examine the performance of C^0 -quadrilateral spectral element method for a model elliptic problem, when one quadrilateral element gradually deforms to a triangular element. Consider

$$(16) \quad -\nabla \cdot (a \nabla u) + bu = f \quad \text{in } \Omega; \quad u|_{\partial\Omega} = g,$$

where a, b, f, g are given smooth functions, and $a \geq a_0 > 0$ for some constant a_0 . To fix the idea, we take Ω to be the polygon in FIG. 2 (leftmost), which is partitioned into three non-overlapping quadrilateral elements. We are concerned with the scenario when the quadrilateral element $AGDE$ gradually degenerates into a triangular element as G moves towards O along FO (see FIG. 2 (middle)).

In the computation, we set the coordinate of the vertex G to be $(-10^{-m}, 0)$ with $m = 3k$, for $k = 1, \dots, 5$, and take the variable coefficients and exact solution to be

$$(17) \quad a(x, y) = x+2, \quad b(x, y) = x+y, \quad u(x, y) = \cos(\pi x) \sin(3y(y-x\sqrt{3}/2+\sqrt{3}/4)).$$

We depict in FIG. 3 the growth of the condition number of the spectral element system and maximum point-wise errors for various N (i.e., N^2 points in each element) and different m . Observe that the condition number grows dramatically as m increases, and the accuracy of the spectral element approximation degrades rapidly when the vertex $G \rightarrow O$. Indeed, the resulted linear system from spectral element discretization becomes nearly singular when G is very close to O .

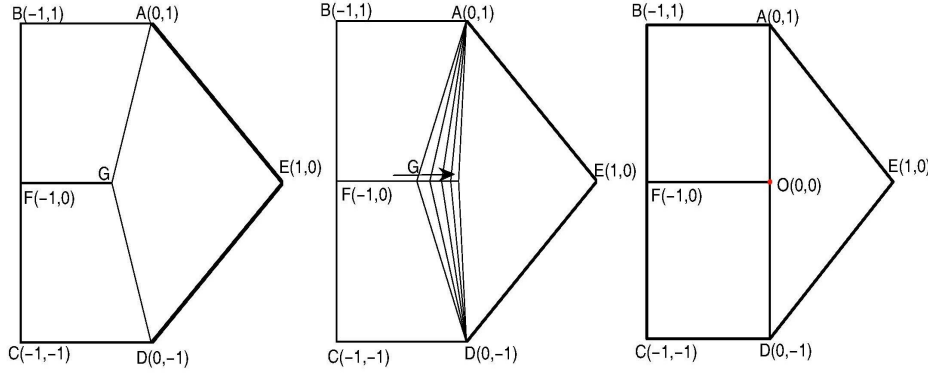


FIGURE 2. Left: domain Ω and its partition; Middle: deformation of a quadrilateral element, where the coordinate of G is $(10^{-m}, 0)$ with $m = 3k, k = 1, \dots, 5$; Right: Ω is divided by the mixture of quadrilaterals and triangle.

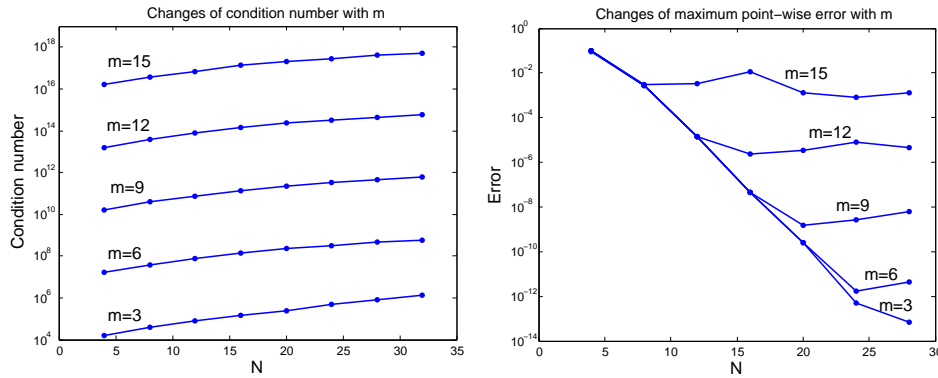


FIGURE 3. Left: variation of condition number of the spectral element system with m ; Right: variation of maximum point-wise error with m for the deforming.

Remark 2.1. *It is important to point out that [7, Thm. 7.1] provided a delicate error estimate with explicit dependance of the errors on the geometric parameters of elements for C^0 -quadrilateral spectral elements for elliptic problems. The error bounds therein contain the powers of $1/J_{\square}^{\min}$ in (10), which tend to infinity in the above limiting process. Therefore, it is necessary to avoid the use of such “bad” elements in practice.*

It is of practical interest to study the extreme case when a quadrilateral element completely reduces to a triangular element (see FIG. 2 (rightmost)). As already mentioned (also see [20]), allowing for some elements to be triangular can lead to much regular mesh and stable spectral element algorithms. Moreover, such a flexibility can facilitate the adaptivity of spectral element methods. Accordingly, it is necessary to develop an algorithm that can handle the singularity with a minimum modification of the standard quadrilateral spectral element codes. This is the theme of our following discussions.

2.3. Triangle-rectangle transformation and analysis of singularity. Suppose that $\theta_4 = \pi$ and $l_3 = l_4$ in FIG. 1 (right), i.e.,

$$(18) \quad x_4 = \frac{x_1 + x_3}{2}, \quad y_4 = \frac{y_1 + y_3}{2}.$$

Then Q deforms to the triangle $\Delta := \Delta Q_1 Q_2 Q_3$, and the transformation (2) reduces to $\mathbf{F}_\Delta : \square \rightarrow \Delta$ given by

$$(19) \quad \mathbf{x} = \mathbf{x}_1 \frac{(1 + \xi)(3 - \eta)}{8} + \mathbf{x}_2 \frac{(1 - \xi)(1 - \eta)}{4} + \mathbf{x}_3 \frac{(3 - \xi)(1 + \eta)}{8}, \quad (\xi, \eta) \in \bar{\square}.$$

With (18), we can further simplify the related geometric quantities. Firstly, the constants in (4) become

$$(20) \quad \begin{aligned} \mathbf{a}_1 &= (3\mathbf{x}_1 + 2\mathbf{x}_2 + 3\mathbf{x}_3)/8, & \mathbf{a}_2 &= (3\mathbf{x}_1 - 2\mathbf{x}_2 - \mathbf{x}_3)/8, \\ \mathbf{a}_3 &= (-\mathbf{x}_1 - 2\mathbf{x}_2 + 3\mathbf{x}_3)/8, & \mathbf{a}_4 &= (-\mathbf{x}_1 + 2\mathbf{x}_2 - \mathbf{x}_3)/8. \end{aligned}$$

In this case, we denote the Jacobian and inverse Jacobi matrices in (6) by \mathbb{J}_Δ and \mathbb{J}_Δ^{-1} , respectively. Note that the Jacobian determinant becomes

$$(21) \quad J_\Delta(\xi, \eta) = \frac{S}{8}(2 - \xi - \eta), \quad \text{where } S = \frac{1}{2} \begin{vmatrix} 1 & 1 & 1 \\ x_3 & x_2 & x_1 \\ y_3 & y_2 & y_1 \end{vmatrix} > 0.$$

In contrast to (10), we have $\min_{(\xi, \eta) \in \bar{\square}} J_\Delta(\xi, \eta) = J_\Delta(1, 1) = 0$. In addition, we have

$$\mathbf{a}_3 + \mathbf{a}_4 = -(\mathbf{a}_2 + \mathbf{a}_4),$$

so the operators $\tilde{\nabla}_a$ and $\tilde{\nabla}_b$ can be simplified to

$$\tilde{\nabla}_a = \alpha(\partial_\xi + \partial_\eta) := \alpha \tilde{\nabla}_+, \quad \tilde{\nabla}_b = \beta(\partial_\xi + \partial_\eta) := \beta \tilde{\nabla}_+,$$

with $\alpha = (x_1 - x_3)/4$ and $\beta = (y_3 - y_1)/4$.

For any $u(x, y)$ on Δ , we define

$$(22) \quad \tilde{u}(\xi, \eta) = (u \circ \mathbf{F}_\Delta)(\xi, \eta), \quad (\xi, \eta) \in \square,$$

and then

$$(23) \quad \tilde{\nabla} \tilde{u} = \mathbb{J}_\Delta \nabla u, \quad \nabla u = \mathbb{J}_\Delta^{-1} \tilde{\nabla} \tilde{u}.$$

Corresponding to (13), the gradient operator in this context can be written as

$$(24) \quad \nabla u = \hat{\nabla} \tilde{u} = J_\Delta^{-1} (\beta \tilde{\nabla}_+ - b_4 \tilde{\nabla}_*, \alpha \tilde{\nabla}_+ + a_4 \tilde{\nabla}_*)^t \tilde{u},$$

Following the principle of deriving the so-called ‘‘pole’’ condition related to the singular mapping in e.g., [17], we require that for $u \in C^1(\bar{\Delta})$, ∇u should be well-defined on \square after transformation. Also notice that for all $(\xi, \eta) \in \square$,

$$(25) \quad 0 < \frac{1 - \xi}{2 - \xi - \eta} < 1, \quad 0 < \frac{1 - \eta}{2 - \xi - \eta} < 1.$$

In view of these, we derive the essential ‘‘pole’’ condition associated with (19):

$$(26) \quad \tilde{\nabla}_+ \tilde{u}(1, 1) = (\partial_\xi \tilde{u} + \partial_\eta \tilde{u})(1, 1) = 0.$$

Accordingly, for any $u, v \in H^1(\Delta)$, we have

$$(27) \quad \begin{aligned} (\nabla u, \nabla v)_\Delta &= \iint_{\square} \hat{\nabla} \tilde{u} \cdot \hat{\nabla} \tilde{v} J_\Delta d\xi d\eta = \frac{8(\alpha^2 + \beta^2)}{S} \iint_{\square} \frac{\tilde{\nabla}_+ \tilde{u} \tilde{\nabla}_+ \tilde{v}}{2 - \xi - \eta} d\xi d\eta \\ &\quad - \frac{8(\beta b_4 - \alpha a_4)}{S} \iint_{\square} \frac{\tilde{\nabla}_+ \tilde{u} \tilde{\nabla}_* \tilde{v} + \tilde{\nabla}_* \tilde{u} \tilde{\nabla}_+ \tilde{v}}{2 - \xi - \eta} d\xi d\eta + \frac{8(a_4^2 + b_4^2)}{S} \iint_{\square} \frac{\tilde{\nabla}_* \tilde{u} \tilde{\nabla}_* \tilde{v}}{2 - \xi - \eta} d\xi d\eta, \end{aligned}$$

and

$$(28) \quad (u, v)_\Delta = (\tilde{u}, J_\Delta \tilde{v})_\square = \frac{S}{8} \iint_\square \tilde{u} \tilde{v} (2 - \xi - \eta) d\xi d\eta.$$

In spectral element discretization, the L^2 -inner product (28) can be computed accurately by usual tensorial Gauss-Lobatto quadrature. However, as demonstrated in Subsection 2.2, the naive approach by the Gaussian quadrature (to avoid sampling the point $(1, 1)$) for (27) significantly degrades the expected spectral accuracy. In this sense, we call point $\mathbf{x} = \mathbf{x}(1, 1)$ (or the counterpart $(\xi, \eta) = (1, 1)$) *the singular point*, and call the edge of Δ on which locating the singular point as *the singular edge*. With an observation of

$$(29) \quad \iint_\square \frac{1}{2 - \xi - \eta} d\xi d\eta = 4 \ln 2,$$

Samson et al [20] developed the spectral element method using modal basis function, which was essential based upon an accurate, recursive formula for evaluating

$$\iint_\square \frac{P_n(\xi) P_m(\eta)}{2 - \xi - \eta} d\xi d\eta,$$

where P_n is the Legendre polynomial of degree n . However, it is more computationally efficient to use nodal basis and numerical integration (27) by the tensorial LGL quadrature.

Thanks to the observation ([17, Lemma 1]) that for any functions u, v in space

$$\mathbb{V}_N^\Delta := \{v : \tilde{v} \in [\mathbb{P}_N]^2, \tilde{\nabla}_+ \tilde{v}(1, 1) = 0\},$$

the value of the integrand $(\widehat{\nabla} \tilde{u} \cdot \widehat{\nabla} \tilde{v}) J_\Delta$ in (27) is zero at singular point $(\xi, \eta) = (1, 1)$, where \mathbb{P}_N was the polynomial space of at most degree N on Λ , a possible way to remove the singularity is choosing \mathbb{V}_N^Δ as the approximation space, and counting the contribution from the singular point to be zero in the numerical integration of (27) by tensorial LGL quadrature. Certainly, if it is feasible, an approximation function with very good approximation property and easy to extend to hybrid meshes in continuous way must be able to be constructed in this space, which is the theme we will discuss in the next section, i.e., the so-called *quasi-interpolation* approximation.

3. Quasi-interpolation approximation on triangle

In this section, we first introduce the quasi-interpolation operator \mathcal{I}_N^Δ on Δ , and then provide the L^2 -error estimate of this interpolation.

3.1. Quasi-interpolation on triangle. Let $\{\xi_j = \eta_j\}_{j=0}^N$ (with $\xi_0 = -\xi_N = -1$) be the Legendre-Gauss-Lobatto (LGL) points on $\bar{\Lambda} = [-1, 1]$, and $\{h_j\}_{j=0}^N$ be the corresponding Lagrange interpolating basis polynomials.

Definition 3.1. For any $u \in C(\bar{\Delta})$ and for Δ with the vertices $\{\mathbf{x}_i\}_{i=1}^3$, we define

$$(30) \quad \tilde{u}(\xi, \eta) = (u \circ \mathbf{F}_\Delta)(\xi, \eta), \quad u_{ij} = \tilde{u}(\xi_i, \eta_j), \quad 0 \leq i, j \leq N,$$

where \mathbf{F}_Δ be the elemental transformation defined by (19). Then the quasi-interpolation of u on Δ is defined by

$$(31) \quad (\mathcal{I}_N^\Delta u)(\mathbf{x}) = (\tilde{\mathcal{I}}_N^\Delta \tilde{u})(\xi, \eta) = \sum_{(i,j) \in \Upsilon_N} u_{ij} \phi_{ij}(\xi, \eta) + \beta_N^\Delta \phi_{NN}(\xi, \eta), \quad \forall \mathbf{x} \in \bar{\Delta},$$

where

$$(32) \quad \phi_{ij}(\xi, \eta) = h_i(\xi) h_j(\eta), \quad \Upsilon_N = \{(i, j) : 0 \leq i, j \leq N, (i, j) \neq (N, N)\},$$

and

$$(33) \quad \beta_N^\Delta = - \sum_{i=0}^{N-1} \frac{u_{iN} + u_{Ni}}{2} \frac{h'_i(1)}{h'_N(1)}.$$

Remark 3.1. Let $\mathbf{x}_{ij} = \mathbf{F}_\Delta(\xi_i, \eta_j)$. One verifies readily that

$$(34) \quad (\mathcal{I}_N^\Delta u)(\mathbf{x}_{ij}) = u(\mathbf{x}_{ij}) = u_{ij}, \quad \forall (i, j) \in \Upsilon_N; \quad (\mathcal{I}_N^\Delta u)(\mathbf{x}_{NN}) = \beta_N^\Delta.$$

Note that β_N^Δ is pre-defined as a weighted average of the nodal values $\{u_{Ni}, u_{iN}\}_{i \neq N}$, which actually provides a very spectrally accurate approximation to the nodal value u_{NN} . For this reason, we call (31) a quasi-interpolation of u , which should be in contrast with the usual interpolation: $\sum_{i,j=0}^N u_{ij} h_i(\xi) h_j(\eta)$ interpolating u at all $\{\mathbf{x}_{ij}\}_{i,j=0}^N$.

Remark 3.2. It is important to point out that the interpolant $\mathcal{I}_N^\Delta u(\mathbf{x})$ satisfies the essential ‘‘pole’’ condition (26), that is,

$$(35) \quad \tilde{\nabla}_+(\tilde{\mathcal{I}}_N^\Delta \tilde{u})(1, 1) = \{\partial_\xi(\tilde{\mathcal{I}}_N^\Delta \tilde{u}) + \partial_\eta(\tilde{\mathcal{I}}_N^\Delta \tilde{u})\}|_{(\xi, \eta)=(1,1)} = 0.$$

Indeed, by definition, we have

$$\begin{aligned} (\tilde{\nabla}_+ \phi_{ij})(1, 1) &= \{h'_i(\xi) h_j(\eta) + h_i(\xi) h'_j(\eta)\}(1, 1) = 0, \quad 0 \leq i, j \leq N-1; \\ (\tilde{\nabla}_+ \phi_{iN})(1, 1) &= (\tilde{\nabla}_+ \phi_{Ni})(1, 1) = h'_i(1), \quad 0 \leq i \leq N-1; \quad (\tilde{\nabla}_+ \phi_{NN})(1, 1) = 2h'_N(1), \end{aligned}$$

so (35) follows from the above, (31) and (33) immediately.

Remark 3.3. Clearly, $\mathcal{I}_N^\Delta u \in \mathbb{V}_N^\Delta$ and $\dim(\mathbb{V}_N^\Delta) = (N+1)^2 - 1$. Li et al [17] constructed a basis $\psi_{ij}(\mathbf{x})$ for \mathbb{V}_N^Δ making use of $\phi_{ij}(\xi, \eta)$, specifically speaking,

$$(36) \quad \psi_{ij}(\mathbf{x}) = \tilde{\psi}_{ij}(\xi, \eta) = \begin{cases} h_i(\xi) h_j(\eta), & 0 \leq i, j \leq N-1, \\ \tilde{h}_i(\xi) h_N(\eta), & 0 \leq i \leq N-1, \\ h_N(\xi) \tilde{h}_j(\eta), & 0 \leq j \leq N-1, \end{cases}$$

where

$$(37) \quad \tilde{h}_j(z) := h_j(z) - \frac{h'_j(1)}{2h'_N(1)} h_N(z).$$

So, the quasi-interpolation can be rewritten as

$$(38) \quad (\mathcal{I}_N^\Delta u)(\mathbf{x}) = (\tilde{\mathcal{I}}_N^\Delta \tilde{u})(\xi, \eta) = \sum_{(i,j) \in \Upsilon_N} u_{ij} \psi_{ij}(\mathbf{x}), \quad \forall \mathbf{x} \in \bar{\Delta}.$$

3.2. Quasi-interpolation error estimate. We analyze the L^2 -error of this interpolation operator. Hereafter, let c be a generic positive constant independent of any function and N , and the expression ‘‘ $A \lesssim B$ ’’ and ‘‘ $A \cong B$ ’’ mean that $A \leq cB$ and $A \lesssim B \lesssim A$, respectively. For a generic positive weight function ω defined on domain Ω , we denote the norm of space $L_\omega^2(\Omega)$ by $\|\cdot\|_{\omega, \Omega}$ and the norm of space $L^\infty(\Omega)$ by $\|\cdot\|_{\infty, \Omega}$. For positive integer r , let $H_\omega^r(\Omega)$ and $H_{0,\omega}^r(\Omega)$ denote the usual weighted Sobolev spaces, whose norm and semi-norm are $\|\cdot\|_{r, \omega, \Omega}$ and $|\cdot|_{r, \omega, \Omega}$ respectively. When $\omega=1$, we drop ω from the notation.

In the following proof, we use the quantities: $W(i, \varrho; r, k)$, $M(i, \varrho; j, \sigma; r, k)$, $B_{r, \Delta}(u)$ and $G_{s, \partial \Delta}(u)$, where $B_{r, \Delta}(u)$ is a quantity with respect to the regularity of u on the interior of Δ and $G_{s, \partial \Delta}(u)$ is a quantity with respect to the regularity of u on the edge of Δ . To avoid distraction from the main results, we put these quantities in Appendix A (see (A.1)-(A.5)).

Theorem 3.1. *If $u \in C^1(\overline{\Delta})$ and $B_{r,\Delta}(u)$, $G_{s,\partial\Delta}(u)$ are finite, then for $2 \leq r, s \leq N+1$,*

$$(39) \quad \|u - \mathcal{I}_N^\Delta u\|_\Delta \lesssim N^{-r} B_{r,\Delta}(u) + N^{-s-2} G_{s,\partial\Delta}(u).$$

Proof. By the triangle inequality, we have

$$(40) \quad \|u - \mathcal{I}_N^\Delta u\|_\Delta \leq \|u - \mathbb{I}_N^\Delta u\|_\Delta + \|\mathbb{I}_N^\Delta u - \mathcal{I}_N^\Delta u\|_\Delta,$$

where

$$\mathbb{I}_N^\Delta u := \tilde{\mathbb{I}}_N^\Delta \tilde{u} = \sum_{i,j=0}^N u_{ij} \phi_{ij}(\xi, \eta)$$

is the usually interpolation on $\overline{\Delta}$. One should note the difference with the quasi-interpolation in (31). We first show that for $r \geq 2$,

$$(41) \quad \|u - \mathbb{I}_N^\Delta u\|_\Delta \lesssim N^{-r} B_{r,\Delta}(u),$$

which can be derived by following the argument for [20, Thm. 4.3], and we sketch its derivation in Appendix A.

The rest of the proof is to deal with the second term in the right-hand side of the inequality (40). By [22, (3.152)],

$$(42) \quad \|v\|_{N,\Lambda} \cong \|v\|_\Lambda, \quad \forall v \in \mathbb{P}_N,$$

where $\|v\|_{N,\Lambda} = (\sum_{j=0}^N v^2(z_j)\omega_j)^{\frac{1}{2}}$ is the discrete norm on the LGL points with $\omega_N = \frac{2}{N(N+1)}$. By (21), (31) and (42), we have

$$(43) \quad \begin{aligned} \|\mathbb{I}_N^\Delta u - \mathcal{I}_N^\Delta u\|_\Delta &\lesssim \|\tilde{\mathbb{I}}_N^\Delta \tilde{u} - \tilde{\mathcal{I}}_N^\Delta \tilde{u}\|_\square \\ &\lesssim |u(\mathbf{x}_{NN}) - \beta_N^\Delta| \|\phi_{NN}\|_\square = |u(\mathbf{x}_{NN}) - \beta_N^\Delta| \|h_N\|_\Lambda^2 \\ &\lesssim |u(\mathbf{x}_{NN}) - \beta_N^\Delta| \|h_N\|_{N,\Lambda}^2 \lesssim \frac{2}{N(N+1)} |u(\mathbf{x}_{NN}) - \beta_N^\Delta|. \end{aligned}$$

Thanks to (26) and (35), we derive

$$(44) \quad \begin{aligned} |(u(\mathbf{x}_{NN}) - \beta_N^\Delta) \cdot \tilde{\nabla}_+ \phi_{NN}(1, 1)| &= |\tilde{\nabla}_+(\tilde{\mathbb{I}}_N^\Delta \tilde{u} - \tilde{u})(1, 1)| \\ &= |\partial_\xi(\tilde{\mathbb{I}}_N^\Delta \tilde{u} - \tilde{u})(\xi, 1)|_{\xi=1} + \partial_\eta(\tilde{\mathbb{I}}_N^\Delta \tilde{u} - \tilde{u})(1, \eta)|_{\eta=1}| \\ &\leq \|\partial_\xi(\tilde{\mathbb{I}}_N^\Delta \tilde{u} - \tilde{u})(\cdot, 1)\|_{\infty,\Lambda} + \|\partial_\eta(\tilde{\mathbb{I}}_N^\Delta \tilde{u} - \tilde{u})(1, \cdot)\|_{\infty,\Lambda}. \end{aligned}$$

According to [22, (3.203)], we have $h'_N(1) = \frac{N(N+1)}{4}$. So,

$$(45) \quad \tilde{\nabla}_+ \phi_{NN}(1, 1) = \partial_\xi h_N(1) + \partial_\eta h_N(1) = \frac{N(N+1)}{2}.$$

Thanks to (45), we derive from (44) that

$$(46) \quad |u(\mathbf{x}_{NN}) - \beta_N^\Delta| \leq \frac{2}{N(N+1)} (\|\partial_\xi(\tilde{\mathbb{I}}_N^\Delta \tilde{u} - \tilde{u})(\cdot, 1)\|_{\infty,\Lambda} + \|\partial_\eta(\tilde{\mathbb{I}}_N^\Delta \tilde{u} - \tilde{u})(1, \cdot)\|_{\infty,\Lambda}).$$

Let \tilde{u}^* be the H^2 -orthogonal projection of the function $\tilde{u}(\xi, 1)$ in \mathbb{P}_N . It is known that for integer $\mu = 0, 1, 2$ and integer $s \geq 2$,

$$(47) \quad \|\tilde{u}(\cdot, 1) - \tilde{u}^*\|_{\mu,\Lambda} \lesssim N^{\mu-s} |\tilde{u}(\cdot, 1)|_{s,\chi^{(s-2,s-2)},\Lambda},$$

where the weight function $\chi^{(\alpha,\beta)} = (1-\xi)^\alpha(1+\xi)^\beta$. By the triangle inequality,

$$(48) \quad \|\partial_\xi(\tilde{\mathbb{I}}_N^\Delta \tilde{u} - \tilde{u})(\cdot, 1)\|_{\infty,\Lambda} \leq \|\partial_\xi(\tilde{\mathbb{I}}_N^\Delta \tilde{u}(\cdot, 1) - \tilde{u}^*)\|_{\infty,\Lambda} + \|\partial_\xi(\tilde{u}(\cdot, 1) - \tilde{u}^*)\|_{\infty,\Lambda}.$$

Using the inverse inequality, the triangle inequality, (A.6) and (47), we have

$$\begin{aligned}
\|\partial_\xi(\mathbb{I}_N^\Delta \tilde{u}(\cdot, 1) - \tilde{u}^*)\|_{\infty, \Lambda} &\lesssim N \|\partial_\xi(\mathbb{I}_N^\Delta \tilde{u}(\cdot, 1) - \tilde{u}^*)\|_\Lambda \\
&\lesssim N(\|\partial_\xi(\mathbb{I}_N^\Delta \tilde{u} - \tilde{u})(\cdot, 1)\|_\Lambda + \|\partial_\xi(\tilde{u}(\cdot, 1) - \tilde{u}^*)\|_\Lambda) \\
(49) \qquad \qquad \qquad &\lesssim N^{2-s} \|\partial_\xi^s \tilde{u}(\cdot, 1)\|_{\chi^{(s-2, s-2)}, \Lambda}.
\end{aligned}$$

We now turn to the second term of (48). By the Sobolev inequality (cf. [22]) and (47),

$$\begin{aligned}
\|\partial_\xi(\tilde{u}(\cdot, 1) - \tilde{u}^*)\|_{\infty, \Lambda} &\lesssim \|\partial_\xi(\tilde{u}(\cdot, 1) - \tilde{u}^*)\|_\Lambda^{1/2} \|\partial_\xi^2(\tilde{u}(\cdot, 1) - \tilde{u}^*)\|_\Lambda^{1/2} \\
&\lesssim N^{\frac{1-s}{2}} \|\partial_\xi^s \tilde{u}(\cdot, 1)\|_{\chi^{(s-2, s-2)}, \Lambda}^{1/2} \cdot N^{\frac{2-s}{2}} \|\partial_\xi^s \tilde{u}(\cdot, 1)\|_{\chi^{(s-2, s-2)}, \Lambda}^{1/2} \\
(50) \qquad \qquad \qquad &\lesssim N^{\frac{3}{2}-s} \|\partial_\xi^s \tilde{u}(\cdot, 1)\|_{\chi^{(s-2, s-2)}, \Lambda}.
\end{aligned}$$

We need consider $\|\partial_\xi^s \tilde{u}(\cdot, 1)\|_{\chi^{(s-2, s-2)}, \Lambda}$. By (A.9) and the basic inequality (A.13),

$$\begin{aligned}
\|\partial_\xi^s \tilde{u}(\cdot, 1)\|_{\chi^{(s-2, s-2)}, \Lambda} &\lesssim \left[\int_{Q_3 Q_4} (1 - \xi^2)^{s-2} \left(\sum_{k=0}^s W(2, \eta; s, k) \partial_x^k \partial_y^{s-k} u \right)^2 dl \right]^{1/2} \\
(51) \qquad \qquad \qquad &\lesssim \sum_{k=0}^s \left\| (1 - \xi^2)^{\frac{s-2}{2}} W(2, \eta; s, k) \partial_x^k \partial_y^{s-k} u \right\|_{Q_3 Q_4}.
\end{aligned}$$

Substituting (49), (50) and (51) into (48) leads to

$$\|\partial_\xi(\mathbb{I}_N^\Delta \tilde{u} - \tilde{u})(\cdot, 1)\|_{\infty, \Lambda} \lesssim N^{2-s} \sum_{k=0}^s \left\| (1 - \xi^2)^{\frac{s-2}{2}} W(2, \eta; s, k) \partial_x^k \partial_y^{s-k} u \right\|_{Q_3 Q_4}.$$

Similarly,

$$\|\partial_\eta(\mathbb{I}_N^\Delta \tilde{u} - \tilde{u})(\cdot, 1)\|_{\infty, \Lambda} \lesssim N^{2-s} \sum_{k=0}^s \left\| (1 - \eta^2)^{\frac{s-2}{2}} W(3, \xi; s, k) \partial_x^k \partial_y^{s-k} u \right\|_{Q_3 Q_4}.$$

Inserting the above two estimates into (46), we get

$$(52) \qquad \qquad \qquad |u(\mathbf{x}_{NN}) - \beta_N^\Delta| \lesssim N^{-s} G_{s, \partial\Delta}(u),$$

so we obtain

$$(53) \qquad \qquad \qquad \|\mathbb{I}_N^\Delta u - \mathcal{I}_N^\Delta u\|_\Delta \lesssim N^{-s-2} G_{s, \partial\Delta}(u).$$

Thus, using (40), (41) and (53) lead to the desired estimate. \square

At this point, we can take \mathbb{V}_N^Δ as the approximation space on Δ , and take the basis function $\psi_{ij}(\mathbf{x})$, $\psi_{mn}(\mathbf{x})$ in (27) to compute the stiffness matrix. As mentioned in Section 2, we count the contribution from the singular point $(\xi, \eta) = (1, 1)$ to be zero in the numerical integration of (27) by tensorial LGL quadrature. Such a treatment of the computation of the singular integral is not only accurate and stable, but also easy to be implemented. Moreover, we will see in next section that the quasi-interpolation on Δ can be easily extended to the quasi-interpolation spectral element approximation on hybrid mesh in the continuous way.

4. Spectral element approximation based on quasi-interpolation

4.1. General setup. Let $\mathcal{T} = \{\Omega_k\}_{k=1}^K$ be a non-overlapping partition of Ω in quadrilateral or triangular elements satisfying the following properties.

- Each vertex of a quadrilateral element is either one of the vertices of the adjacent element, or the midpoint (the singular point) of the adjacent triangular element.

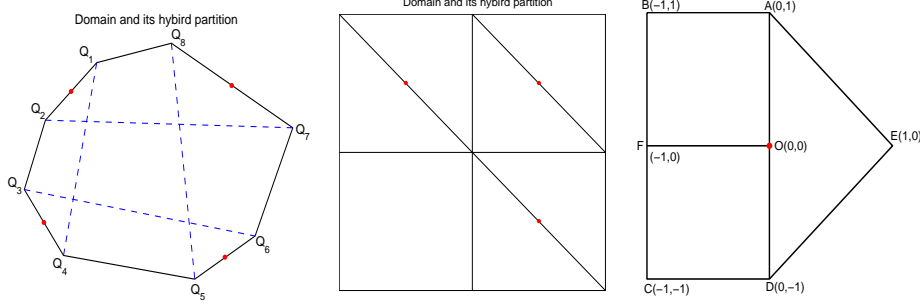


FIGURE 4. Illustration of partition of a given domain Ω . Left: Ω and its hybrid partition with 9 elements; Middle: Ω and its hybrid partition with 7 elements; Right: Ω and its hybrid partition with 3 elements.

- There exist positive constants α_0 and α_1 such that every inner angle $\theta_{k,\nu}$ of any element Ω_k satisfies: $0 < \alpha_0 \leq \theta_{k,\nu} \leq \alpha_1 < \pi$, where $k = 1, 2, \dots, K$, $\nu = 1, 2, 3$ or $\nu = 1, 2, 3, 4$.
- There exists a constant κ independent of any element $\Omega_k \in \mathcal{T}$ such that

$$\sup_{\Omega_k \in \mathcal{T}} \frac{h_{\Omega_k}}{\gamma_{\Omega_k}} \leq \kappa < \infty,$$

where h_{Ω_k} and γ_{Ω_k} are the length of the longest and the shortest edge of the element Ω_k , respectively.

In general, we hybridise the elements in three scenarios: the singular points locating on $\partial\Omega$ (see FIG. 4 (leftmost)), locating between two triangular elements (see FIG. 4 (middle)), and locating between a triangle and two quadrilaterals (see FIG. 4 (rightmost)), where the “.” denotes the singular points.

To this end, we denote by Ω_τ the set of all singular points on $\bar{\Omega}$, and let K_τ be the total number of the points in Ω_τ . Denote by \mathbf{F}_k the mappings from \square to Ω_k , $1 \leq k \leq K$, when Ω_k is a quadrilater, \mathbf{F}_k refers to \mathbf{F}_\square , and when Ω_k is a triangle, \mathbf{F}_k refers to \mathbf{F}_\triangle . Then the approximation space on Ω is defined as

$$\mathbb{V}_{N,\mathcal{T}}^\Omega := \{v : v \in H^1(\Omega), v|_{\Omega_k} \circ \mathbf{F}_k \in [\mathbb{P}_N]^2, \text{ and } v \text{ satisfies (26) at all } \mathbf{x} \in \Omega_\tau\}.$$

We next introduce the basis. For this purpose, we define the mapped LGL point set Ω_N on $\bar{\Omega}$ as

$$\Omega_N := \{\mathbf{x} : \mathbf{x} = \mathbf{F}_k(\xi_i, \eta_j), 1 \leq k \leq K, 0 \leq i, j \leq N\},$$

where $\{(\xi_i, \eta_j), 0 \leq i, j \leq N\}$ are the LGL points on $\bar{\square}$. Let N_Ω be the total number of points in Ω_N , and we rewrite Ω_N as

$$\Omega_N = \{\mathbf{x} : \mathbf{x} = \mathbf{x}_\lambda = (x_\lambda, y_\lambda), \lambda = 1, 2, \dots, N_\Omega\},$$

where $\lambda = \lambda(i, j, k)$, $i, j = 0, 1, 2, \dots, N$; $k = 1, 2, \dots, K$ is the index mapping from the local ordinal number of the point $\mathbf{F}_k(\xi_i, \eta_j)$ on $\bar{\Omega}_k$ to the global ordinal number of this point on $\bar{\Omega}$. A basis of $\mathbb{V}_{N,\mathcal{T}}^\Omega$ can be built by splicing together the imagines of all the local basis (36). More precisely, letting Ω_e be the set of all LGL points locating on the singular edges, corresponding to LGL point $\mathbf{x}_\lambda \in \Omega_N \setminus \Omega_e$, we define

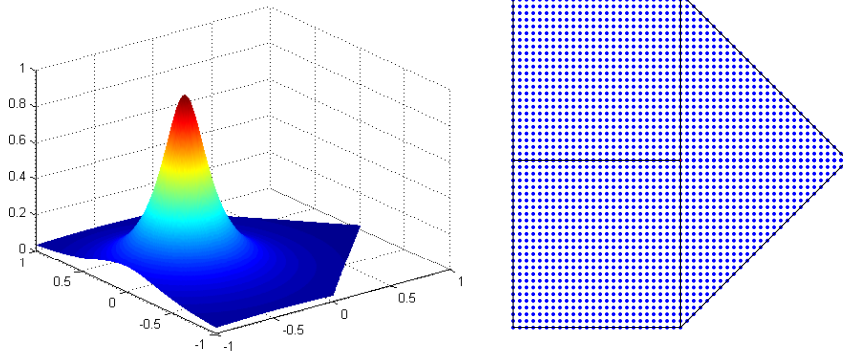


FIGURE 5. Left: the two dimensional Runge-type function $u(x, y) = 1/(1 + 25(x + 1/2)^2 + 25y^2)$; Right: the uniform grids on Ω .

the basis function as

$$\varphi_\lambda(\mathbf{x}) = \begin{cases} \phi_{ij} \circ \mathbf{F}_k^{-1}, & \mathbf{x} \in \bar{\Omega}_k, \\ 0, & \text{elsewhere.} \end{cases}$$

Corresponding to LGL point $\mathbf{x}_\lambda \in \Omega_e \setminus \Omega_\tau$, the basis function is

$$\varphi_\lambda(\mathbf{x}) = \begin{cases} (\tilde{h}_i(\xi)h_N(\eta)) \circ \mathbf{F}_k^{-1} \text{ or } (h_N(\xi)\tilde{h}_j(\eta)) \circ \mathbf{F}_k^{-1}, & \mathbf{x} \in \bar{\Omega}_k, \\ 0, & \text{elsewhere.} \end{cases}$$

Note that $\dim(\mathbb{V}_{N,\mathcal{T}}^\Omega) = N_\Omega - K_\tau$. With the basis, we define the assembled quasi-interpolation hybrid spectral element approximation as

$$(54) \quad \mathcal{I}_N^\Omega v := \sum_{\lambda=1}^{N_\Omega - K_\tau} v_\lambda \varphi_\lambda,$$

where $v_\lambda = v(\mathbf{x}_\lambda)$, $\mathbf{x}_\lambda \in \Omega_N \setminus \Omega_\tau$. Then we have $\mathcal{I}_N^\Omega v \in \mathbb{V}_{N,\mathcal{T}}^\Omega$.

As a numerical illustration, we consider the Runge-type function (see [24, Fig. 1]):

$$(55) \quad u(x, y) = 1/(1 + 25(x + 1/2)^2 + 25y^2), \quad (x, y) \in \bar{\Omega},$$

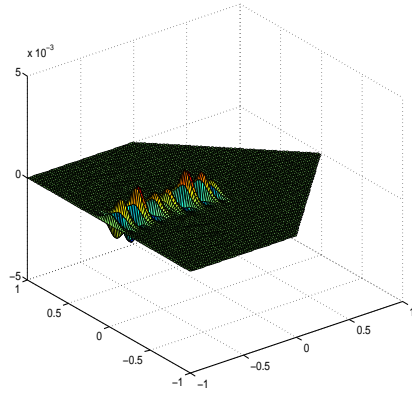
where Ω is the polygon with the partition in FIG. 2 (rightmost). In FIG. 5 (left), we plot the Runge-type function (55) over the domain Ω . In FIG. 6 (a) to (f), we plot the point-wise errors $u - \mathcal{I}_N^\Omega u$ on a uniform mesh with spacing 0.025 in both directions (see FIG. 5 (right)) for various N . We see that the quasi-interpolation provides a stable and accurate approximation of u , and the deformation of a quadrilateral element to a triangular element does not degrade the accuracy.

4.2. Spectral element scheme for an elliptic model problem. A weak formulation of (16) with $g = 0$ is to find $u \in H_0^1(\Omega)$ such that

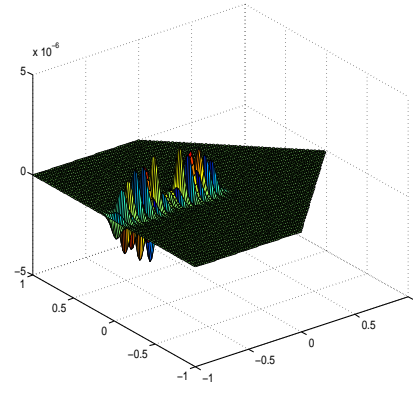
$$(56) \quad (a\nabla u, \nabla v)_\Omega + (bu, v)_\Omega = (f, v)_\Omega, \quad \forall v \in H_0^1(\Omega).$$

The spectral element scheme for (56) is to find $u_N \in \mathbb{V}_{N,\mathcal{T}}^{\Omega,0} := \mathbb{V}_{N,\mathcal{T}}^\Omega \cap H_0^1(\Omega)$ such that

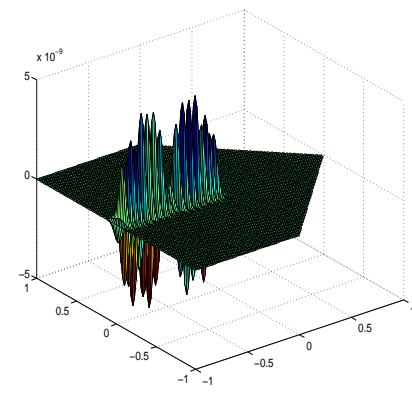
$$(57) \quad (a\nabla u_N, \nabla v_N)_\Omega + (bu_N, v_N)_\Omega = (f, v_N)_\Omega, \quad \forall v_N \in \mathbb{V}_{N,\mathcal{T}}^{\Omega,0}.$$



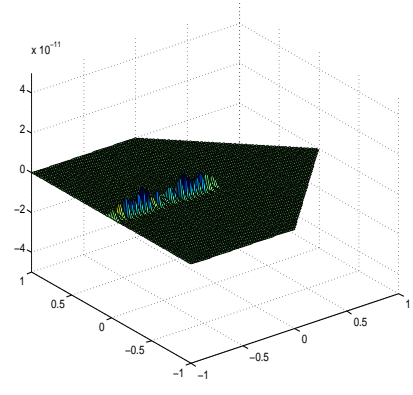
(a) $N=16$



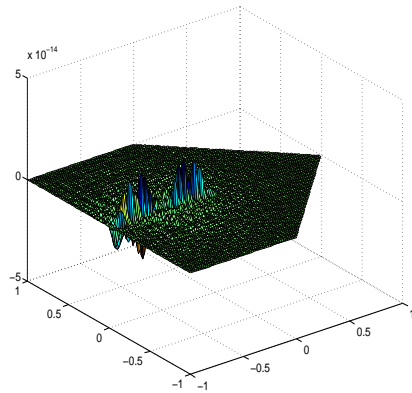
(b) $N=32$



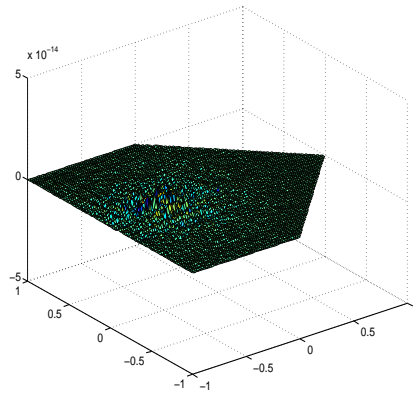
(c) $N=48$



(d) $N=64$



(e) $N=80$



(f) $N=96$

FIGURE 6. The point-wise approximation errors (measured on uniform mesh) of the quasi-interpolation $\mathcal{I}_N^\Omega u$ with various N .

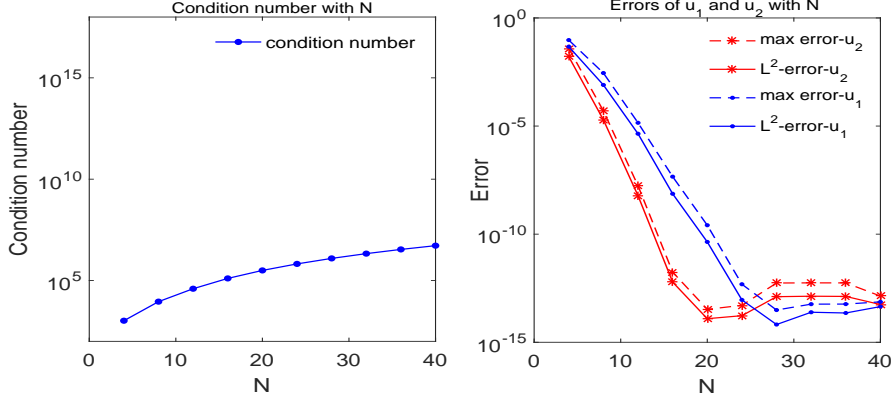


FIGURE 7. Results of Test 1. Left: condition number of the hybrid SEM with different N ; Right: the variations of the maximum point-wise and L^2 -errors with N .

Corresponding to the three typical local hybrid partition in FIG. 4, we give the following three numerical experiments to test this hybrid SEM for the elliptic problem.

• **Test 1.** We first consider the problem (16) with Ω and its partition as in FIG. 4 (rightmost). Here, we take $a = x + 2, b = x + y$, and the exact solutions respectively to be

$$u_1 = \cos(\pi x) \sin\left(3y\left(y - \frac{\sqrt{3}}{2}x + \frac{\sqrt{3}}{4}\right)\right); \quad u_2 = \sin\left(\pi x + \frac{\pi}{4}\right) \sin\left(\pi y + \frac{\pi}{4}\right).$$

FIG. 7 shows the condition number of the spectral element system against N (left) and the decay of the maximum point-wise and the discrete L^2 -errors with different N (right).

• **Test 2.** We next consider the problem (16) with Ω and its hybrid partition as in FIG. 4 (middle). In the test, we take $a = 1, b = 1$, and the exact solutions to be u_2 in Test 1 and

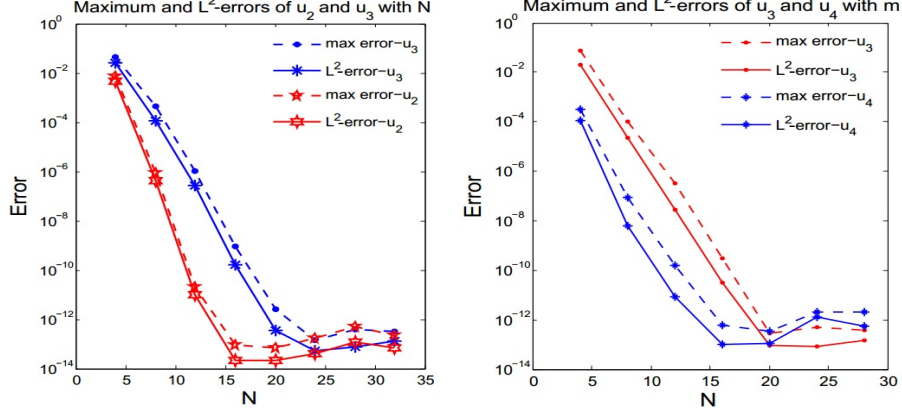
$$u_3 = e^{x+y-1} \sin\left(3y\left(y - \frac{\sqrt{3}}{2}x + \frac{\sqrt{3}}{4}\right)\right),$$

respectively. We plot in FIG. 8 (left) the maximum point-wise and the discrete L^2 -errors for various N .

• **Test 3.** Consider the elliptic problem with mixed boundary conditions:

$$(58) \quad \begin{cases} -\operatorname{div}(a\nabla u) + bu = f, & \text{in } \Omega, \\ u = h, \text{ on } \Gamma_D; \quad \frac{\partial u}{\partial \mathbf{n}} = g, & \text{on } \Gamma_N, \end{cases}$$

where the Neumann boundary is along $\Gamma_N := \bigcup_{i=4}^7 Q_i Q_{i+1}$, and the Dirichlet boundary is along $\Gamma_D = \partial\Omega \setminus \Gamma_N$. Here, Ω has a hybrid partition as in FIG. 4 (leftmost). Again, we take $a = x + 2, b = x + y$, and the exact solutions to be u_3 in Test 2, and $u_4 = (2 - x - y)^{\frac{5}{2}} e^{xy-1}$, respectively. FIG. 8 (right) shows the decay of the maximum point-wise and discrete L^2 -errors against N .

FIGURE 8. Errors against N (left: Test 2; right: Test 3).

We see that the spectral accuracy of our approach can be achieved for all three cases, which should be in distinctive contrast with the number results observed from FIG. 3.

4.3. Error analysis. We now analyse the convergence of the scheme (57). For simplicity, assume $a(x, y) = b(x, y) = 1$. As mentioned before, the local partition containing triangular elements actually has three typical situations (see FIG. 4). Here, we focus on the situation where the singular point is so-called hanging node (singular point lies between a triangle and two quadrilaterals, see FIG. 4 (right-most)), as the other two cases are much easier to analyze.

Consider Ω with a partition \mathcal{T} in FIG. 4 (rightmost). For clarity, denote by \square_{12} and \triangle the quadrilateral $ABCD$ and the triangle $\triangle ADE$, respectively. For any integer $r \geq 2$, we define the space

$$\mathbb{V}_{\bar{\tau}}^r(\Omega) := \{u : u \in H_0^1(\Omega), u|_{\square_{12}} \in H^r(\square_{12}), u|_{\triangle} \in H^r(\triangle)\}.$$

Then we have the following error estimate.

Theorem 4.1. *Let u and u_N be the solutions of (56) and (57), respectively. If $u \in \mathbb{V}_{\bar{\tau}}^r(\Omega)$ with $2 \leq r \leq N + 1$, then*

$$\|u - u_N\|_{1,\Omega} \lesssim N^{1-r} (|u|_{r,\square_{12}} + |u|_{r,\triangle}).$$

We next make necessary preparations to prove this theorem. Introduce two orthogonal projections ${}_0\pi_{N,\xi}^1$ and $\pi_{N,\eta}^{1,0}$ on Λ_ξ and Λ_η , respectively. Define

$${}_0H^1(\Lambda) = \{v : v(-1) = 0, v \in H^1(\Lambda)\}; \quad {}_0\mathbb{P}_N = {}_0H^1(\Lambda) \cap \mathbb{P}_N; \quad \mathbb{P}_N^0 = H_0^1(\Lambda) \cap \mathbb{P}_N.$$

For any $v \in {}_0H^1(\Lambda_\xi)$, ${}_0\pi_{N,\xi}^1 v \in {}_0\mathbb{P}_N$ is the ${}_0H^1$ -orthogonal projection defined by

$$(\partial_\xi(v - {}_0\pi_{N,\xi}^1 v), \partial_\xi w)_{\Lambda_\xi} = 0, \quad \forall w \in {}_0\mathbb{P}_N.$$

For $v \in H_0^1(\Lambda_\eta)$, $\pi_{N,\eta}^{1,0} v \in \mathbb{P}_N^0$ is the H_0^1 -orthogonal projection defined by

$$(\partial_\eta(v - \pi_{N,\eta}^{1,0} v), \partial_\eta w)_{\Lambda_\eta} = 0, \quad \forall w \in \mathbb{P}_N^0.$$

Denote

$$\Gamma_0 = \{(x, \pm 1) : -1 \leq x \leq 0\} \cup \{(-1, y) : -1 \leq y \leq 1\},$$

and

$$H_{\Gamma_0}^1(\square_{12}) = \{v : v \in H^1(\square_{12}), v|_{\Gamma_0} = 0\}.$$

For any function $v \in H_{\Gamma_0}^1(\square_{12})$, the approximation polynomial of v is defined by

$${}_0\Pi_{N,\square_{12}}^1 v := ({}_0\pi_{N,\xi}^1 \circ \pi_{N,\eta}^{1,0} \tilde{v}) \circ \mathbf{F}_{\square}^{-1},$$

where $\mathbf{F}_{\square} : \square \rightarrow \square_{12}$ is the transformation (5) with $Q = \square_{12}$.

Lemma 4.1. *If $v \in H_{\Gamma_0}^1(\square_{12}) \cap H^r(\square_{12})$, then for $2 \leq r \leq N + 1$,*

$$(59) \quad \|v - {}_0\Pi_{N,\square_{12}}^1 v\|_{1,\square_{12}} \lesssim N^{1-r} |v|_{r,\square_{12}}.$$

Proof. It is sufficient to prove it with $\square_{12} = \square$. By the Poincarè inequality, one has

$$(60) \quad \|\tilde{v} - {}_0\pi_{N,\xi}^1 \circ \pi_{N,\eta}^{1,0} \tilde{v}\|_{1,\square} \lesssim \|\nabla(\tilde{v} - {}_0\pi_{N,\xi}^1 \circ \pi_{N,\eta}^{1,0} \tilde{v})\|_{\square}.$$

By the triangle inequality,

$$(61) \quad \|\partial_{\xi}(\tilde{v} - {}_0\pi_{N,\xi}^1 \circ \pi_{N,\eta}^{1,0} \tilde{v})\|_{\square}^2 \lesssim \|\partial_{\xi}(\tilde{v} - {}_0\pi_{N,\xi}^1 \tilde{v})\|_{\square}^2 + \|\partial_{\xi}({}_0\pi_{N,\xi}^1(\tilde{v} - \pi_{N,\eta}^{1,0} \tilde{v}))\|_{\square}^2.$$

By [7, (3.5)], for $\mu = 0, 1$,

$$(62) \quad \|\partial_{\eta}^{\mu}(\tilde{v} - \pi_{N,\eta}^{1,0} \tilde{v})\|_{\square} \lesssim N^{\mu-r} \|\partial_{\eta}^r \tilde{v}\|_{L^2(\Lambda_{\xi}, L_{\chi}^{2(r-1, r-1)}(\Lambda_{\eta}))}.$$

From [9, Thm. 3.2], we can derive that for $\mu = 0, 1$,

$$(63) \quad \|\partial_{\xi}^{\mu}(\tilde{v} - {}_0\pi_{N,\xi}^1 \tilde{v})\|_{\square} \lesssim N^{\mu-r} \|\partial_{\xi}^r \tilde{v}\|_{L_{\chi}^{2(r-1, r-1)}(\Lambda_{\xi}, L^2(\Lambda_{\eta}))}.$$

By (63) with $\mu = 1$, we have

$$(64) \quad \|\partial_{\xi}(\tilde{v} - {}_0\pi_{N,\xi}^1 \tilde{v})\|_{\square}^2 \lesssim N^{2-2r} \|\partial_{\xi}^r \tilde{v}\|_{L_{\chi}^{2(r-1, r-1)}(\Lambda_{\xi}, L^2(\Lambda_{\eta}))}^2 \lesssim N^{2-2r} |\tilde{v}|_{r,\square}^2.$$

By (63) with $\mu = r = 1$, and by (62) with $\mu = 0$, we have

$$(65) \quad \begin{aligned} \|\partial_{\xi}({}_0\pi_{N,\xi}^1(\tilde{v} - \pi_{N,\eta}^{1,0} \tilde{v}))\|_{\square}^2 &\lesssim \|\partial_{\xi}(\tilde{v} - \pi_{N,\eta}^{1,0} \tilde{v})\|_{\square}^2 \lesssim N^{2-2r} \|\partial_{\xi} \partial_{\eta}^{r-1} \tilde{v}\|_{L^2(\Lambda_{\xi}, L_{\chi}^{2(r-2, r-2)}(\Lambda_{\eta}))}^2 \\ &\lesssim N^{2-2r} |\tilde{v}|_{r,\square}^2. \end{aligned}$$

We derive from (61)-(65) that

$$(66) \quad \|\partial_{\xi}(\tilde{v} - {}_0\pi_{N,\xi}^1 \circ \pi_{N,\eta}^{1,0} \tilde{v})\|_{\square}^2 \lesssim N^{2-2r} |\tilde{v}|_{r,\square}^2.$$

In a similar way, we can obtain

$$(67) \quad \|\partial_{\eta}(\tilde{v} - {}_0\pi_{N,\xi}^1 \circ \pi_{N,\eta}^{1,0} \tilde{v})\|_{\square}^2 \lesssim N^{2-2r} |\tilde{v}|_{r,\square}^2.$$

Using (60), (66) and (67) leads to

$$\|\tilde{v} - {}_0\pi_{N,\xi}^1 \circ \pi_{N,\eta}^{1,0} \tilde{v}\|_{1,\square} \lesssim N^{1-r} |\tilde{v}|_{r,\square}.$$

This ends the proof. \square

We next construct an approximation polynomial on Δ . Define

$$\hat{\Delta} := \{(\hat{x}, \hat{y}) : 0 < \hat{x}, \hat{y}, \hat{x} + \hat{y} < 1\}, \quad \mathbb{P}_{N,\hat{\Delta}}^{\hat{\Delta}} := \text{span}\{\hat{x}^k \hat{y}^l : 0 \leq k, l, k+l \leq N\}.$$

Recall that there exists an invertible linear mapping $\mathbf{M}_{\Delta} : \hat{\Delta} \rightarrow \Delta$, which maps the reference triangle $\hat{\Delta}$ onto Δ . Denote $\mathbb{P}_{N,\Delta}^{\Delta} = \mathbb{P}_{N,\hat{\Delta}}^{\hat{\Delta}} \circ \mathbf{M}_{\Delta}^{-1}$. According to [21, (4.5)], for any function $\hat{v} \in H^2(\hat{\Delta})$, there exists an orthogonal projection $\Pi_{N,\hat{\Delta}}^{-1,-1,-1} \hat{v} \in \mathbb{P}_{N,\hat{\Delta}}^{\hat{\Delta}}$ defined by

$$\langle \hat{v} - \Pi_{N,\hat{\Delta}}^{-1,-1,-1} \hat{v}, \hat{w} \rangle_{\hat{\Delta}} = 0, \quad \forall \hat{w} \in \mathbb{P}_{N,\hat{\Delta}}^{\hat{\Delta}},$$

where

$$\begin{aligned} \langle \hat{v}, \hat{w} \rangle_{\hat{\Delta}} &= (\partial_{\hat{x}}(\partial_{\hat{y}} - \partial_{\hat{x}})\hat{v}, \partial_{\hat{x}}(\partial_{\hat{y}} - \partial_{\hat{x}})\hat{w})_{\hat{x}, \hat{\Delta}} + (\partial_{\hat{y}}(\partial_{\hat{y}} - \partial_{\hat{x}})\hat{v}, \partial_{\hat{y}}(\partial_{\hat{y}} - \partial_{\hat{x}})\hat{w})_{\hat{y}, \hat{\Delta}} \\ &\quad + (\partial_{\hat{y}}\hat{v}, \partial_{\hat{y}}\hat{w})_{\hat{\Gamma}_1} + (\partial_{\hat{x}}\hat{v}, \partial_{\hat{x}}\hat{w})_{\hat{\Gamma}_2} + \hat{v}(0, 0)\hat{w}(0, 0), \end{aligned}$$

with

$$\hat{\Gamma}_1 = \{(0, \hat{y}) : 0 < \hat{y} < 1\}; \quad \hat{\Gamma}_2 = \{(\hat{x}, 0) : 0 < \hat{x} < 1\}.$$

For any $v \in H^2(\Delta)$, we define the approximation polynomial on Δ as $\Pi_{N,\Delta}^{-1,-1,-1}v := (\Pi_{N,\Delta}^{-1,-1,-1}\hat{v}) \circ \mathbf{M}_{\Delta}^{-1}$. Apparently, $\Pi_{N,\Delta}^{-1,-1,-1}v \in \mathbb{P}_N^{\Delta}$. According to [21, Lemma 5.1] and [21, Lemma 4.3], we have the following property and estimate.

Lemma 4.2. *Suppose $v \in H^r(\Delta)$ with $r \geq 2$, and $v|_{DE} = v|_{AE} = 0$. Then*

(68)

$$(i) \quad (\Pi_{N,\Delta}^{-1,-1,-1}v)|_{AD} = \pi_{N,\eta}^{1,0}(v|_{AD}); \quad (ii) \quad \|\nabla(v - \Pi_{N,\Delta}^{-1,-1,-1}v)\|_{\Delta} \lesssim N^{1-r}|v|_{r,\Delta}.$$

At this point, we are able to glue the approximation polynomial on \square_{12} and Δ into the global approximation function $\Pi_{N,\tau}^{1,0}u$, which is defined by

$$\Pi_{N,\tau}^{1,0}u =: \begin{cases} 0\Pi_{N,\square_{12}}^1(u|_{\square_{12}}), & \text{on } \square_{12}, \\ \Pi_{N,\Delta}^{-1,-1,-1}(u|_{\Delta}), & \text{on } \Delta. \end{cases}$$

This global approximation function enjoys the following property.

Lemma 4.3. *For any $u \in \mathbb{V}_{\tau}^r(\Omega)$ with $2 \leq r \leq N+1$, we have*

(69)

$$(i) \quad \Pi_{N,\tau}^{1,0}u \in \mathbb{V}_{N,\mathcal{T}}^{\Omega,0};$$

(70)

$$(ii) \quad \|u - \Pi_{N,\tau}^{1,0}u\|_{1,\Omega} \lesssim N^{1-r}(|u|_{r,\square_{12}} + |u|_{r,\Delta}).$$

Proof. Since $\Pi_{N,\Delta}^{-1,-1,-1}(u|_{\Delta})$ is differentiable on $\bar{\Delta}$, we infer from (i) of [20, Proposition 2.1], that the polynomial $\Pi_{N,\Delta}^{-1,-1,-1}(u|_{\Delta})$ belongs to \mathbb{V}_N^{Δ} . For the continuity of $\Pi_{N,\tau}^{1,0}u$ on Ω , (i) of Lemma 4.2 ensures its continuity across AD , so that continuous on Ω . Thus, we have proved (i). One can easily derive (ii) from Lemma 4.1 and (ii) of Lemma 4.2 together with the Poincaré inequality on Δ (cf. [10, Remark 4.1]). \square

With the above preparations, we are ready to prove Theorem 4.1.

Proof of Theorem 4.1. Denoting $a(u, v) := (\nabla u, \nabla v)_{\Omega} + (u, v)_{\Omega}$, by (56) and (57), we obtain

$$a(u - u_N, v_N) = 0, \quad \forall v_N \in \mathbb{V}_{N,\mathcal{T}}^{\Omega,0}.$$

Furthermore, we have

$$\|u - u_N\|_{1,\Omega}^2 = a(u - u_N, u - v_N) \leq \|u - u_N\|_{1,\Omega} \|u - v_N\|_{1,\Omega},$$

i.e.,

(71)

$$\|u - u_N\|_{1,\Omega} \leq \|u - v_N\|_{1,\Omega}, \quad \forall v_N \in \mathbb{V}_{N,\mathcal{T}}^{\Omega,0}.$$

Taking $v_N = \Pi_{N,\tau}^{1,0}u$ in (71), and using (ii) of Lemma 4.3, we obtain the desired estimate.

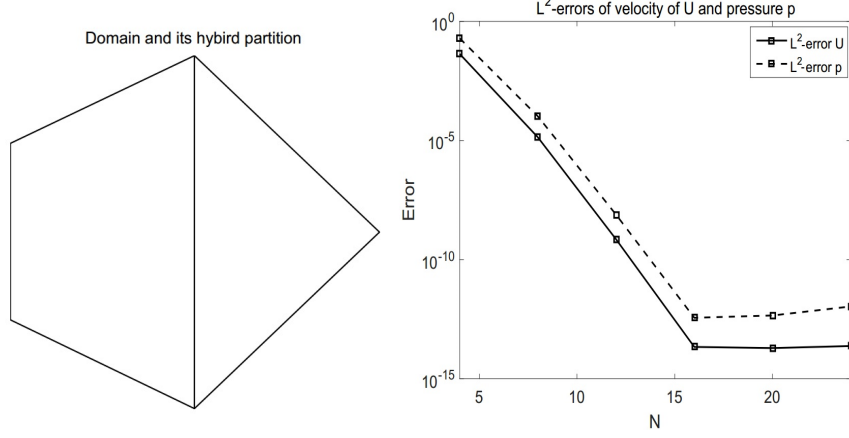


FIGURE 9. Left: Ω with its hybrid partition; Right: L^2 -errors of velocity \mathbf{u} and pressure p with N .

4.4. Application to the Stokes equation. Hereafter, we apply the hybrid SEM to the steady Stokes problem:

$$(72) \quad \begin{cases} -\Delta \mathbf{u} + \nabla p = \mathbf{f}, & \text{in } \Omega, \\ \nabla \cdot \mathbf{u} = 0, & \text{in } \Omega, \\ \mathbf{u} = 0, & \text{on } \partial\Omega, \end{cases}$$

where $\mathbf{f} \in [L^2(\Omega)]^2$.

In what follows, we denote $Y = H_0^1(\Omega)$ and $\mathbf{Y} = Y^2$. Introduce the bilinear form:

$$A(\mathbf{u}, \mathbf{v}) = \iint_{\Omega} \nabla \mathbf{u} \nabla \mathbf{v} \, dx dy, \quad \forall \mathbf{u}, \mathbf{v} \in \mathbf{Y}.$$

Let

$$X := \left\{ q : q \in L^2(\Omega), \iint_{\Omega} q \, dx dy = 0 \right\}.$$

Define the bilinear form on $\mathbf{Y} \times X$:

$$b(\mathbf{v}, p) = - \iint_{\Omega} \nabla \cdot \mathbf{v} p \, dx dy, \quad \forall \mathbf{v} \in \mathbf{Y}, \quad \forall p \in X.$$

Thus, the weak formulation for the Stokes equations (72) is to find $\mathbf{u} \in \mathbf{Y}$ and $p \in X$ such that

$$(73) \quad \begin{cases} A(\mathbf{u}, \mathbf{v}) + b(\mathbf{v}, p) = (\mathbf{f}, \mathbf{v})_{\Omega}, & \forall \mathbf{v} \in \mathbf{Y}, \\ b(\mathbf{u}, q) = 0, & \forall q \in X. \end{cases}$$

Assume that Ω is a polygon with a hybrid partition \mathcal{T} . Denoting $Y_N = Y \cap \mathbb{V}_{N, \mathcal{T}}^{\Omega, 0}$ and $\mathbf{Y}_N = Y_N^2$, to present the spectral element scheme, we also need define the approximate space X_N of X . Let $\{l_i, i = 1, 2, \dots, N-1\}$ be the usual Lagrangian interpolation polynomials associating to the $N-1$ interior LGL points in Λ . Then $\{l_i(\xi)l_j(\eta), i, j = 1, 2, \dots, N-1\}$ are the nodal basis functions of the space $[\mathbb{P}_{N-2}]^2$. And, we define the global nodal basis functions of $X_N(\Omega)$ as

$$(74) \quad \rho_{\mu}(\mathbf{x}) = \begin{cases} (l_i(\xi)l_j(\eta)) \circ \mathbf{F}_k^{-1}, & \mathbf{x} \in \bar{\Omega}_k, \\ 0, & \text{elsewhere,} \end{cases}$$

where $\mu = \mu(i, j, k)$, $i, j = 1, 2, \dots, N-1$; $k = 1, 2, \dots, K$ is the index mapping from the local ordinal number to the global ordinal number. Thus

$$X_N(\Omega) = \text{span}\{\rho_\mu : \mu = 1, 2, \dots, K(N-1)^2\} \cap X.$$

where $L_0^2(\Omega) = \{u \in L^2(\Omega) : (u, 1)_\Omega = 0\}$ is the subspace of L^2 -functions with zero mean on Ω . Thus, the SEM for (73) is to find $\mathbf{u}_N \in \mathbf{Y}_N$ and $p_N \in X_N$ such that

$$(75) \quad \begin{cases} A(\mathbf{u}_N, \mathbf{v}_N) + b(\mathbf{v}_N, p_N) = (\mathbf{f}, \mathbf{v}_N)_\Omega, & \forall \mathbf{v}_N \in \mathbf{Y}_N, \\ b(\mathbf{u}_N, q_N) = 0, & \forall q_N \in X_N. \end{cases}$$

Remark 4.1. *It is known that in order to avoid the spurious pressure modes, in the discrete scheme of the Stokes equations, the discrete velocity and pressure spaces are required to satisfy the inf-sup condition (see [18, 1, 2]). To this end, similar to the usual $\mathbb{P}_N \times \mathbb{P}_{N-2}$ approach in the rectangular spectral method, we take the pressure approximation space X_N to be two “degrees” fewer than the velocity approximation space \mathbf{Y}_N .*

We next present some numerical results obtained by the hybrid SEM, where the domain Ω is partitioned as in FIG. 9 (left). In the test, we take the exact solution to be $\mathbf{u}(x, y) = (\sin x \cos y, -\cos x \sin y)^T$ and $p(x, y) = \sin x \sin y$. We plot in FIG. 9 (right) the discrete L^2 -errors for velocity $\mathbf{u}(x, y)$ and pressure p with N . We observe the spectral convergence for both \mathbf{u} and p .

Acknowledgments

The research was supported by NSFC Grants 11571224 and 11571225, and partially supported by Singapore MOE AcRF Tier 1 Grants (RG15/12 and RG27/15), and Singapore MOE AcRF Tier 2 Grant (MOE 2013-T2-1-095, ARC 44/13).

Appendix A. Proof of (41)

We first give the definitions of $W(i, \varrho; r, k)$, $M(i, \varrho; j, \sigma; r, k)$, $B_{r, \Delta}(u)$ and $G_{s, \partial\Delta}(u)$. Define

$$(A.1) \quad W(i, \varrho; r, k) = (a_i + a_4 \varrho)^k (b_i + b_4 \varrho)^{r-k}, \quad 0 \leq k \leq r,$$

where $(i, \varrho) = (2, \eta)$ or $(3, \xi)$. Further denote

$$(A.2) \quad M(i, \varrho; j, \sigma; r, k) = \begin{cases} W(i, \varrho; r-1, 0)(b_j + b_4 \sigma), & k = 0, \\ W(i, \varrho; r-1, k-1)(a_j + a_4 \sigma) + W(i, \varrho; r-1, k)(b_j + b_4 \sigma), & 1 \leq k \leq r-1, \\ W(i, \varrho; r-1, r-1)(a_j + a_4 \sigma), & k = r, \end{cases}$$

where $(i, \varrho; j, \sigma) = (2, \eta; 3, \xi)$ or $(3, \xi; 2, \eta)$. Define

$$(A.3) \quad B_{2, \Delta}(u) = \sum_{k=0}^2 \left(\|(1 + \xi)^{\frac{1}{2}} W(2, \eta; 2, k) \partial_x^k \partial_y^{2-k} u\|_\Delta + \|(1 + \eta)^{\frac{1}{2}} W(3, \xi; 2, k) \partial_x^k \partial_y^{2-k} u\|_\Delta \right) + |u|_{2, J_{\Delta}^{-1}, \Delta} + |u|_{1, J_{\Delta}^{-1}, \Delta},$$

and for $r \geq 3$,

$$\begin{aligned}
(A.4) \quad B_{r,\Delta}(u) &= \sum_{k=0}^r \left(\|(1-\xi)^{\frac{r-2}{2}}(1+\xi)^{\frac{r-1}{2}}W(2,\eta;r,k)\partial_x^k\partial_y^{r-k}u\|_{\Delta} \right. \\
&\quad + \|(1-\eta)^{\frac{r-2}{2}}(1+\eta)^{\frac{r-1}{2}}W(3,\xi;r,k)\partial_x^k\partial_y^{r-k}u\|_{\Delta} \\
&\quad \left. + \|(1-\xi)^{\frac{r-3}{2}}(1+\xi)^{\frac{r-2}{2}}M(2,\eta;3,\xi;r,k)\partial_x^k\partial_y^{r-k}u\|_{\Delta} \right) \\
&\quad + \sum_{k=0}^{r-1} \left(\|(1-\xi)^{\frac{r-3}{2}}(1+\xi)^{\frac{r-2}{2}}\partial_{\eta}W(2,\eta;r-1,k)\partial_x^k\partial_y^{r-1-k}u\|_{\Delta} \right).
\end{aligned}$$

Finally, we define

$$\begin{aligned}
(A.5) \quad G_{s,\partial\Delta}(u) &= \sum_{k=0}^s \left(\|(1-\xi^2)^{\frac{s-2}{2}}W(2,\eta;s,k)\partial_x^k\partial_y^{s-k}u\|_{Q_3Q_4} \right. \\
&\quad \left. + \|(1-\eta^2)^{\frac{s-2}{2}}W(3,\xi;s,k)\partial_x^k\partial_y^{s-k}u\|_{Q_3Q_4} \right).
\end{aligned}$$

We now prove (41). By [22, Thm. 3.44], we know that for any $v \in H^r(\Lambda)$ with $1 \leq r \leq N+1$ and $\mu = 0, 1$,

$$(A.6) \quad \|v - I_N^{\xi}v\|_{\mu,\Lambda} \lesssim N^{\mu-r}|v|_{r,\chi^{(r-1,r-1)},\Lambda}.$$

Let I_d be the identity operator. Then by (21) and (A.6), we have

$$\begin{aligned}
(A.7) \quad \|u - \mathbb{I}_N^{\Delta}u\|_{\Delta} &\lesssim \|\tilde{u} - \tilde{\mathbb{I}}_N^{\Delta}\tilde{u}\|_{\square} = \|\tilde{u} - I_N^{\xi}I_N^{\eta}\tilde{u}\|_{\square} \\
&\lesssim \|(I_d - I_N^{\xi})(I_d - I_N^{\eta})\tilde{u} - (I_d - I_N^{\xi})\tilde{u} - (I_d - I_N^{\eta})\tilde{u}\|_{\square} \\
&\lesssim \|(I_d - I_N^{\xi})(I_d - I_N^{\eta})\tilde{u}\|_{\square} + \|(I_d - I_N^{\xi})\tilde{u}\|_{\square} + \|(I_d - I_N^{\eta})\tilde{u}\|_{\square} \\
&\lesssim N^{-1}\|(I_d - I_N^{\xi})\partial_{\eta}\tilde{u}\|_{\square} + \|(I_d - I_N^{\xi})\tilde{u}\|_{\square} + \|(I_d - I_N^{\eta})\tilde{u}\|_{\square} \\
&\lesssim N^{-r}(\|(1-\xi^2)^{(r-2)/2}\partial_{\xi}^{r-1}\partial_{\eta}\tilde{u}\|_{\square} \\
&\quad + \|(1-\xi^2)^{(r-1)/2}\partial_{\xi}^r\tilde{u}\|_{\square} + \|(1-\eta^2)^{(r-1)/2}\partial_{\eta}^r\tilde{u}\|_{\square}).
\end{aligned}$$

We next transform the variables (ξ, η) back to (x, y) . For clarity, we denote

$$\begin{aligned}
(A.8) \quad E_{r,\square}^{(1)}(\tilde{u}) &= \|(1-\xi^2)^{(r-1)/2}\partial_{\xi}^r\tilde{u}\|_{\square}, \quad E_{r,\square}^{(2)}(\tilde{u}) = \|(1-\eta^2)^{(r-1)/2}\partial_{\eta}^r\tilde{u}\|_{\square}, \\
E_{r,\square}^{(3)}(\tilde{u}) &= \|(1-\xi^2)^{(r-2)/2}\partial_{\xi}^{r-1}\partial_{\eta}\tilde{u}\|_{\square}.
\end{aligned}$$

A direct calculation from (19) yields

$$\begin{aligned}
\partial_{\xi}x &= a_2 + a_4\eta, \quad \partial_{\xi}y = b_2 + b_4\eta, \quad \partial_{\eta}x = a_3 + a_4\xi, \quad \partial_{\eta}y = b_3 + b_4\xi, \\
\partial_{\xi}\tilde{u} &= (a_2 + a_4\eta)\partial_x u + (b_2 + b_4\eta)\partial_y u, \quad \partial_{\eta}\tilde{u} = (a_3 + a_4\xi)\partial_x u + (b_3 + b_4\xi)\partial_y u.
\end{aligned}$$

Thus, we have

$$\begin{aligned}
\partial_\xi^r \tilde{u} &= \sum_{k=0}^r \binom{r}{k} (a_2 + a_4 \eta)^k (b_2 + b_4 \eta)^{r-k} \partial_x^k \partial_y^{r-k} u, \\
\partial_\eta^r \tilde{u} &= \sum_{k=0}^r \binom{r}{k} (a_3 + a_4 \xi)^k (b_3 + b_4 \xi)^{r-k} \partial_x^k \partial_y^{r-k} u, \\
\partial_\xi^{r-1} \partial_\eta \tilde{u} &= \partial_\eta \sum_{k=0}^{r-1} \binom{r}{k} (a_2 + a_4 \eta)^k (b_2 + b_4 \eta)^{r-1-k} \partial_x^k \partial_y^{r-1-k} u \\
&= \sum_{k=0}^{r-1} \binom{r-1}{k} (a_2 + a_4 \eta)^k (b_2 + b_4 \eta)^{r-1-k} \\
&\quad \cdot \{ (a_3 + a_4 \xi) \partial_x^{k+1} \partial_y^{r-1-k} u + (b_3 + b_4 \xi) \partial_x^k \partial_y^{r-k} u \} \\
&\quad + \sum_{k=0}^{r-1} \binom{r-1}{k} \partial_\eta \{ (a_2 + a_4 \eta)^k (b_2 + b_4 \eta)^{r-1-k} \} \partial_x^k \partial_y^{r-1-k} u,
\end{aligned} \tag{A.9}$$

where the constants a_i, b_i are defined in (20). By (21) and (25), we derive that for $r \geq 3$,

$$\begin{aligned}
E_{r,\square}^{(1)}(\tilde{u}) &= \left(\iint_{\square} (\partial_\xi^r \tilde{u})^2 (1 - \xi^2)^{r-1} d\xi d\eta \right)^{\frac{1}{2}} \\
&\lesssim \sum_{k=0}^r \left\| (1 - \xi)^{\frac{r-2}{2}} (1 + \xi)^{\frac{r-1}{2}} W(2, \eta; r, k) \partial_x^k \partial_y^{r-k} u \right\|_{\Delta},
\end{aligned} \tag{A.10}$$

$$\begin{aligned}
E_{r,\square}^{(2)}(\tilde{u}) &= \left(\iint_{\square} (\partial_\eta^r \tilde{u})^2 (1 - \eta^2)^{r-1} d\xi d\eta \right)^{\frac{1}{2}} \\
&\lesssim \sum_{k=0}^r \left\| (1 - \eta)^{\frac{r-2}{2}} (1 + \eta)^{\frac{r-1}{2}} W(3, \xi; r, k) \partial_x^k \partial_y^{r-k} u \right\|_{\Delta},
\end{aligned} \tag{A.11}$$

$$\begin{aligned}
E_{r,\square}^{(3)}(\tilde{u}) &= \left(\iint_{\square} (\partial_\xi^{r-1} \partial_\eta \tilde{u})^2 (1 - \xi^2)^{r-2} d\xi d\eta \right)^{\frac{1}{2}} \\
&\lesssim \sum_{k=0}^r \left(\left\| (1 - \xi)^{\frac{r-3}{2}} (1 + \xi)^{\frac{r-2}{2}} M(2, \eta; 3, \xi; r, k) \partial_x^k \partial_y^{r-k} u \right\|_{\Delta} \right. \\
&\quad \left. + \sum_{k=0}^{r-1} \left\| (1 - \xi)^{\frac{r-3}{2}} (1 + \xi)^{\frac{r-2}{2}} \partial_\eta W(2, \eta; r-1, k) \partial_x^k \partial_y^{r-1-k} u \right\|_{\Delta} \right).
\end{aligned} \tag{A.12}$$

In the above derivations, we used the basic inequality

$$\sigma_1^2 + \sigma_2^2 + \cdots + \sigma_r^2 \leq (\sigma_1 + \sigma_2 + \cdots + \sigma_r)^2 \leq r(\sigma_1^2 + \sigma_2^2 + \cdots + \sigma_r^2), \tag{A.13}$$

with $\sigma_i \geq 0$, $i = 1, 2, \dots, r$.

For $r = 2$, we derive from a direct calculation that

$$\begin{aligned}
\|\partial_\xi \partial_\eta \tilde{u}\|_{\square} &\lesssim |u|_{2, J_{\Delta}^{-1}, \Delta} + |u|_{1, J_{\Delta}^{-1}, \Delta}, \\
\|(1 - \xi^2)^{1/2} \partial_\xi^2 \tilde{u}\|_{\square} &\lesssim \sum_{k=0}^2 \left\| (1 + \xi)^{\frac{1}{2}} W(2, \eta; 2, k) \partial_x^k \partial_y^{2-k} u \right\|_{\Delta}, \\
\|(1 - \eta^2)^{1/2} \partial_\eta^2 \tilde{u}\|_{\square} &\lesssim \sum_{k=0}^2 \left\| (1 + \eta)^{\frac{1}{2}} W(3, \xi; 2, k) \partial_x^k \partial_y^{2-k} u \right\|_{\Delta}.
\end{aligned} \tag{A.14}$$

Finally, we obtain (41) from (A.7)-(A.14).

References

- [1] C. Bernardi and Y. Maday. Spectral methods. *Handbook of Numerical Analysis*, 5:209–485, 1997.
- [2] C. Canuto, M. Hussaini, A. Quarteroni, and T. Zang. *Spectral Methods*. Scientific Computation. Springer, Berlin, 2007.
- [3] Q. Chen and I. Babuška. Approximate optimal points for polynomial interpolation of real functions in an interval and in a triangle. *Comp. Meth. Appl. Math. Eng.*, 128(2)(1995)405–417.
- [4] L. Chen, J. Shen and C. Xu. A triangular spectral method for stokes equations. *Numer. Math.: Theory, Methods Appl.*, 4(2011)158–179.
- [5] M. Deville, P. Fischer, and E. Mund. *High-Order Methods for Incompressible Fluid Flow*, volume 9 of Cambridge Monographs on Applied and Computational Mathematics. Cambridge University Press, Cambridge, 2002.
- [6] M. Dubiner. Spectral methods on triangles and other domains. *J. Sci. Comput.*, 6(4)(1991)345–390.
- [7] B. Guo and H. Jia. Spectral method on quadrilaterals. *Math. Comp.*, 79(272)(2010)2237–2264.
- [8] B. Guo and H. Jia. Pseudospectral method for quadrilaterals. *J. Comput. Appl. Math.*, 236(5)(2011)962–979.
- [9] B. Guo and L. Wang. Jacobi approximations in non-uniformly Jacobi-weighted Sobolev spaces. *J. Approx. Theory*, 128(1)(2004)1–41.
- [10] B. Guo and L. Wang. Error analysis of spectral method on a triangle. *Adv. Comput. Math.*, 26(4)(2007)473–496.
- [11] J. Hesthaven. From electrostatics to almost optimal nodal sets for polynomial interpolation in a simplex. *SIAM J. Numer. Anal.*, 35(2)(1998)655–676.
- [12] H. Jia and B. Guo. Petrov-Galerkin spectral element method for mixed inhomogeneous boundary value problems on polygons. *Chin. Ann. Math. Ser. B*, 31(6)(2010)855–878.
- [13] G. Karniadakis and S. Sherwin. *Spectral/hp element methods for computational fluid dynamics*. Numerical Mathematics and Scientific Computation. Oxford University Press, New York, second edition, 2005.
- [14] T. Koornwinder. Two-variable analogues of the classical orthogonal polynomials. In *theory and application of special functions (Proc. Advanced Sem., Math. Res. Center, Univ. Wisconsin, Madison, Wis., 1975)*, pages 435–495. Math. Res. Center, Univ. Wisconsin, Publ. No. 35. Academic Press, New York, 1975.
- [15] H. Li and J. Shen. Optimal error estimates in Jacobi-weighted Sobolev spaces for polynomial approximations on the triangle. *Math. Comp.*, 79(271)(2010)1621–1646.
- [16] H. Li and L. Wang. A spectral method on tetrahedra using rational basis functions. *Int. J. Numer. Anal. Model.*, 7(2)(2010)330–355.
- [17] Y. Li, L. Wang, H. Li, and H. Ma. A new spectral method on triangles. *Spectral and high order methods for partial differential equations*, volume 76 of *Lect. Notes Comput. Sci. Eng.*, pages 237–246. Springer, Heidelberg, 2011.
- [18] Y. Maday, A. T. Patera, and E. M. Ronquist. A well-posed optimal spectral element approximation for the stokes problem. *ICASE Report*, (1987)48–87.
- [19] A. Patera. A spectral element method for fluid dynamics: laminar flow in a channel expansion. *Journal of Computational Physics*, 54(3)(1984)468–488.
- [20] M. Samson, H. Li, and L. Wang. A new triangular spectral element method I: implementation and analysis on a triangle. *Numer. Algorithms*, 64(3)(2013)519–547.
- [21] W. Shan and H. Li. The triangular spectral element method for stokes eigenvalues. Accepted by *Math. Comp.*, 2016.
- [22] J. Shen, T. Tang, and L. Wang. *Spectral Methods: Algorithms, Analysis and Applications*, volume 41. Springer Science & Business Media, 2011.
- [23] J. Shen, L. Wang, and H. Li. A triangular spectral element method using fully tensorial rational basis functions. *SIAM J. Numer. Anal.*, 47(3)(2009)1619–1650.
- [24] S. Sherwin and G. Karniadakis. A triangular spectral element method; applications to the incompressible Navier-Stokes equations. *Comput. Methods Appl. Mech. Engrg.*, 123(1-4)(1995)189–229.
- [25] G. Strang and G. Fix. *An Analysis of the Finite Element Method*, volume 212. Prentice-hall Englewood Cliffs, NJ, 1973.

- [26] M. Taylor, B. Wingate, and R. Vincent. An algorithm for computing Fekete points in the triangle. *SIAM J. Numer. Anal.*, 38(5)(2000)1707–1720.

Department of Mathematics, College of Sciences, Shanghai University, Shanghai 200444, China
and Zhangjiagang Campus, Jiangsu University of Science and Technology, Jiangsu 215600, China
E-mail: `fxlj1@just.edu.cn`

Department of Mathematics, College of Sciences, Shanghai University, Shanghai 200444, China
E-mail: `hpm@shu.edu.cn`

Division of Mathematical Sciences, School of Physical and Mathematical Sciences, Nanyang
Technological University, 637371, Singapore
E-mail: `LiLian@ntu.edu.sg`

Department of Mathematics, College of Sciences, Shanghai University, Shanghai 200444, China
E-mail: `hwu@staff.shu.edu.cn`